FDTD Investigations into UWB Radar Technique of Breast Tumor Detection and Location

Hua Wang, Marek E. Bialkowski, Feng Liu and Stuart Crozier
The University of Queensland, School of Information Technology and Electrical Engineering, St Lucia (Queensland), Australia
Email: {hwang, meb, feng, stuart} @itee.uq.edu.au

Abstract

In this paper, a finite difference time domain (FDTD) method is applied to investigate capabilities of an ultra-wide band (UWB) radar system to detect and locate a breast tumor. The first part of these investigations concerns a phantom formed by a circular cylindrical plastic container with liquid and a small highly reflecting target. In the second part, a three-dimensional numerical breast model is used to perform more advanced studies. In all of the carried out FDTD simulations, a quasi-plane wave is used as an incident wave. Various time snap shots of the electromagnetic field are recorded to learn about the physical phenomenon of reflection and scattering in different layers of the phantoms. The obtained results should form the ground for working out suitable guidelines for designing an optimal microwave breast imaging apparatus based on the UWB radar technique.

1. Introduction

Recently, various passive and active microwave techniques have been proposed as a viable alternative to X-ray mammography for early detection of breast cancer. These include: passive microwave radiometry [1], [2], hybrid microwave-induced acoustic imaging [3], microwave tomography [4] and ultra-wideband microwave radar technique [5-10]. The passive microwave radiometry relies on temperature differences between malignant and normal breast tissue. The hybrid approach uses ultrasound transducers to detect pressure waves generated by tumor expansion due to microwave heating. In the tomographic approach, a nonlinear inverse scattering problem is solved to obtain spatial distribution of dielectric properties in the breast. The ultra wideband microwave radar uses short duration pulses to detect the presence and location of significant backscatter from malignant tissue.

The basis for the active microwave techniques of breast cancer detection and location is the significant contrast in dielectric properties of normal and malignant breast tissue at this particular frequency spectrum [11-13]. At this frequency range tumours and muscle tissues rich of water exhibit higher dielectric properties than low water contained tissues such as fat forming the major part of normal breast tissue. For the normal breast tissues, dielectric properties vary only ±10% around the relative permittivity ε_r = 9 and the conductivity σ = 0.4 S/m. For the malignant tumours, the relative permittivity is about 50 and the conductivity is approximately 7 S/m.

An UWB microwave radar technique for detecting and locating a breast tumour is the subject of investigations in this paper. We emulate the operation of a practical UWB imaging system which is based on a step-frequency synthesized pulse technique [5], [6], [8], [9], [10]. This system consists of a wideband microwave source, a mechanical or electronic antenna scanner, a receiver and a PC controller/processor. In this system the time domain pulse is obtained via stepping frequency over a wide frequency band. A receiver performs measurements of reflection coefficient in frequency domain and its time/space domain equivalent is obtained by applying an Inverse FFT. In the mechanical scanning system, measurements are repeated for various locations of a UWB probe antenna. In its electronic equivalent, this function is performed by activating electronically various UWB array antenna elements. Next, an image is created by combining all of the processed results coming from different transmitting/receiving antenna locations. In order to enhance the detection process various signal detection enhancement techniques such as confocal microwave imaging [5], space-time beamforming [6] or time-reverse wave focusing [7] can be employed. Because the microwave imaging involves a number of undesired phenomena such as internal reflections in antenna elements, reflections and scattering at the interface between an antenna and an imaged object as well as due to its non uniform structure, it is important to carry out full EM analysis of these processes using realistic phantoms. The results of such an analysis can be useful to work out guidelines for designing and developing an

optimal UWB radar imaging system for breast cancer detection.

2. Methodology

In the work presented here, we apply a finite difference time domain (FDTD) method [14] to obtain visualization of reflection and scattering in various layers of the breast phantom. The choice of the FDTD method is motivated by the fact that it has a distinct advantage of handling field-sample interactions in the time domain. An understanding of these interactions becomes of significant importance, as microwave imaging is moving towards the search of better signal to noise ratio (SNR) and image resolution. In the results presented in this paper, two cases are considered. One is in which, the breast is modeled by a simple phantom in the form of a plastic circular cylindrical container with liquid and a highly reflecting target. The second phantom is a breast phantom obtained from detailed MR images. Each of them is illuminated by a quasi plane wave. In practice this kind of illumination can be achieved using a large horn antenna or a planar array of in-phase fed wide band antenna elements. Images of field distribution at different time snap shots are collected to the purpose of investigating the wave incidence, reflection and scattering.

2.1. FDTD method

The mathematical model of the FDTD method is based on Faraday and Ampere's laws which provide a system of equations that form an independent set of coupled relationships between time-varying electric and magnetic fields. The FDTD method resolves these equations in the time domain by applying central differences to time and space derivatives.

$$H_x\big|_{i,j+1/2,k+1/2}^{n+1/2} = C_{h1} H_x\big|_{i,j+1/2,k+1/2}^{n} + C_{h2}\left(\frac{E_y\big|_{i,j+1/2,k+1}^{n} - E_y\big|_{i,j+1/2,k}^{n}}{\Delta z} - \frac{E_z\big|_{i,j+1,k+1/2}^{n} - E_z\big|_{i,j,k+1/2}^{n}}{\Delta y}\right)$$

$$H_y\big|_{i+1/2,j,k+1/2}^{n+1/2} = C_{h1} H_y\big|_{i+1/2,j,k+1/2}^{n} + C_{h2}\left(\frac{E_z\big|_{i+1,j,k+1/2}^{n} - E_z\big|_{i,j,k+1/2}^{n}}{\Delta x} - \frac{E_x\big|_{i+1/2,j,k+1}^{n} - E_x\big|_{i+1/2,j,k}^{n}}{\Delta z}\right)$$

$$H_z\big|_{i+1/2,j+1/2,k}^{n+1/2} = C_{h1} H_z\big|_{i+1/2,j+1/2,k}^{n} + C_{h2}\left(\frac{E_x\big|_{i+1/2,j+1,k}^{n} - E_x\big|_{i+1/2,j,k}^{n}}{\Delta y} - \frac{E_y\big|_{i+1,j+1/2,k}^{n} - E_y\big|_{i,j+1/2,k}^{n}}{\Delta x}\right)$$

$$E_x\big|_{i+1/2,j,k}^{n+1} = C_{e1} E_x\big|_{i+1/2,j,k}^{n} + \frac{\Delta t}{\varepsilon} J_x\big|_{i+1/2,j,k}^{n+1/2} + C_{e2}\left(\frac{H_z\big|_{i+1/2,j+1/2,k}^{n+1/2} - H_z\big|_{i+1/2,j-1/2,k}^{n+1/2}}{\Delta y} - \frac{H_y\big|_{i+1/2,j,k+1/2}^{n+1/2} - H_y\big|_{i+1/2,j,k-1/2}^{n+1/2}}{\Delta y}\right)$$

$$E_y\big|_{i,j+1/2,k}^{n+1} = C_{e1} E_y\big|_{i,j+1/2,k}^{n} + \frac{\Delta t}{\varepsilon} J_y\big|_{i,j+1/2,k}^{n+1/2} + C_{e2}\left(\frac{H_x\big|_{i,j+1/2,k+1/2}^{n+1/2} - H_x\big|_{i,j+1/2,k-1/2}^{n+1/2}}{\Delta z} - \frac{H_z\big|_{i+1/2,j+1/2,k}^{n+1/2} - H_z\big|_{i-1/2,j+1/2,k}^{n+1/2}}{\Delta x}\right)$$

$$E_z\big|_{i,j,k+1/2}^{n+1} = C_{e1} E_y\big|_{i,j,k+1/2}^{n} + \frac{\Delta t}{\varepsilon} J_y\big|_{i,j,k+1/2}^{n+1/2} + C_{e2}\left(\frac{H_y\big|_{i+1/2,j,k+1/2}^{n+1/2} - H_y\big|_{i-1/2,j,k+1/2}^{n+1/2}}{\Delta x} - \frac{H_x\big|_{i,j+1/2,k+1/2}^{n+1/2} - H_x\big|_{i,j-1/2,k+1/2}^{n+1/2}}{\Delta y}\right)$$

$$C_{h1} = 1, \quad C_{h2} = \frac{\Delta t}{\mu}, \quad C_{e1} = \frac{2\varepsilon - \sigma\Delta t}{2\varepsilon + \sigma\Delta t}, \quad C_{e2} = \frac{2\Delta t}{(2\varepsilon + \sigma\Delta t)}$$

In the discrete FDTD computational domain in Cartesian coordinates, the dimensions of the Yee cell are defined by Δx, Δy and Δz, as small as 0.5 mm to reduce the "staircase" error [15] on the curved surface of plastic container and copper. The relative permeability $\mu_r(x, y, z)$, relative permittivity $\varepsilon_r(x, y, z)$ and material conductivity $\sigma(x, y, z)$ are defined at the center of each cell are stored in a look-up table for the purpose of efficient memory utilization. Finally, Berenger's PML (Perfectly Matched Layer) [16] is developed to handle an absorbing boundary condition. In addition, the Message Passing Interface (MPI) library [17] is used so that a parallel computing frame is implemented. As a result of these steps, the simulation process for each of the two investigated cases takes less than 20 mins on a cluster of three servers each with 2 XEON 3.6 GHz processors. The results are generated and visualized by recording the electric fields at various positions in real time. By using this approach, the details of wave propagation, reflection and scattering can be analysed. In particular, this EM field analysis can allow for investigating the subtle features of the detection of very small targets.

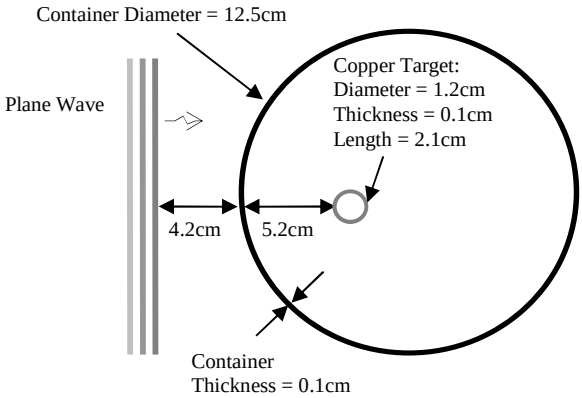

Figure 1. The configuration of a plastic container with liquid and a highly reflecting target, as used in an experimental setup described in [18].

2.2. System model

The FDTD model used here emulates a planar microwave imaging system [18] that employs a synthesized pulse technique. The FDTD model for the first analysed phantom that includes a plastic container and a small highly reflecting target is shown in Fig.1.

In the experimental system, reflection coefficient measurements are performed in the frequency domain over an assumed wide frequency band for many locations of a probe antenna over a planar surface. For each location of the probe, the measured data is transformed to the time domain by using an Inverse FFT. In the FDTD model a quasi planar wave is launched having a constant power spectral density over the assumed wide frequency band.

Fig.2. shows a relationship between the frequency domain and time domain representations of the signal incident on the imaged object.

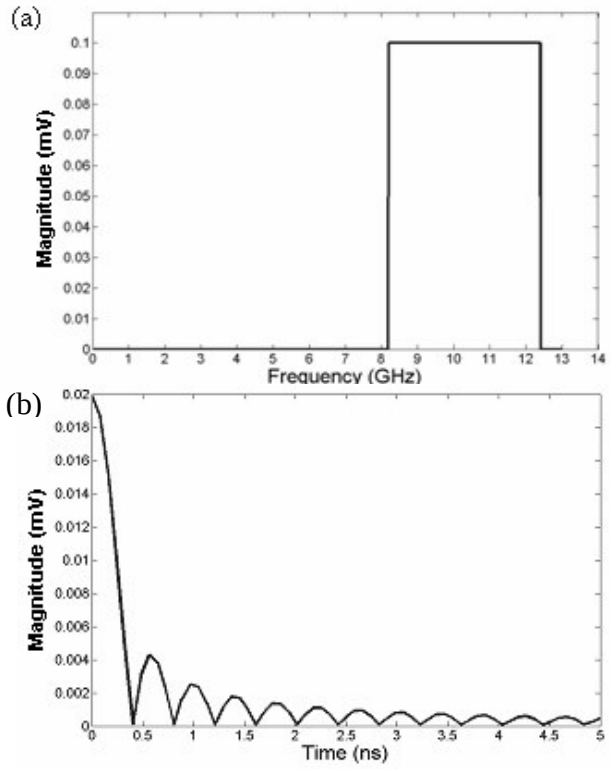

Figure 2. Synthesized pulse, (a) frequency domain (b) time domain representation.

Note that in the current experimental system, as described in [18], the frequency band is assumed to be between 8.4 to 12.4 GHz. Both FDTD simulations and the experimental setup are easily extendable to a larger frequency band to obtain a higher resolution of target location.

In the first experimental setup, shown in Fig.1, the imaged object consists of a circular cylindrical plastic container (ε_r=2.5) with a diameter of 12.5cm with thickness of 1mm. The container is assumed to be filled with oil (ε_r=4.0). A highly conductive object (σ=1e6), in the form of copper pipe of diameter 1.2cm and length of 2.1 cm located close to the centre of the plastic container represents a tumour.

In the second experiment, a detailed breast phantom obtained from an MR image is investigated. This phantom contains the outside skin to observe the dominant reflection from the skin, while the internal area is filled with breast fat, and a spherical tumour tissue with 6mm diameter is located inside. The dielectric properties are ε_r=6.89, σ=32.25 for skin, ε_r=0.67, σ=4.0 for breast fat and ε_r=9.19, σ=44.12 for malignant tissue, which is equivalent to muscle tissue. A pulse, as shown in Fig.2b, is launched towards the phantom, from the side in the first case and from the top in the second case.

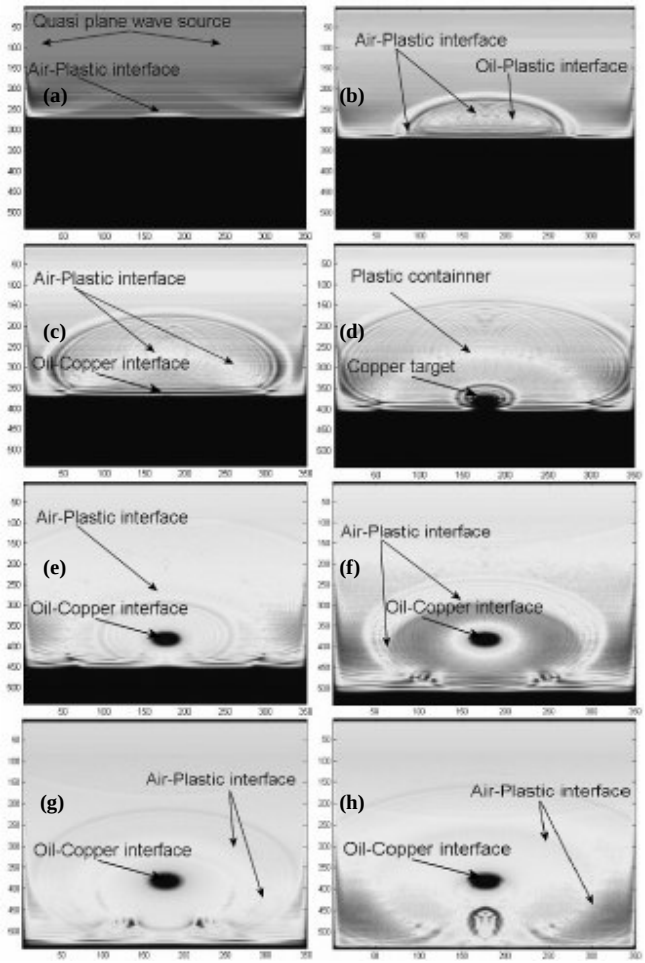

Figure 3. Time snap shots showing the process of wave propagation in the first phantom.

3. Results and discussion

The obtained FDTD simulation results allow for animation of the entire process of wave launching, propagation, reflection and scattering. Here, we present only selected time snap shots of the field distribution representing this animated process.

Fig. 3 illustrates the incidence, reflection and scattering phenomenon at different layers of the first phantom. Fig. 3 (a) shows the wave propagation in free space prior to the incidence on the plastic container. A major reflection at the plastic container interface is observed in Fig. 3(b). Fig. 3(c) shows the field distribution before the wave strikes the copper target. In the next slides, the wave reflection and scattering process from the target takes place.

Before the reflected and scattered waves reach the outside region of the phantom, an additional reflection and scattering phenomenon at the inner interface between the liquid and the plastic container takes place. This additional scattering obscures the capability of target detection from the outside of the phantom.

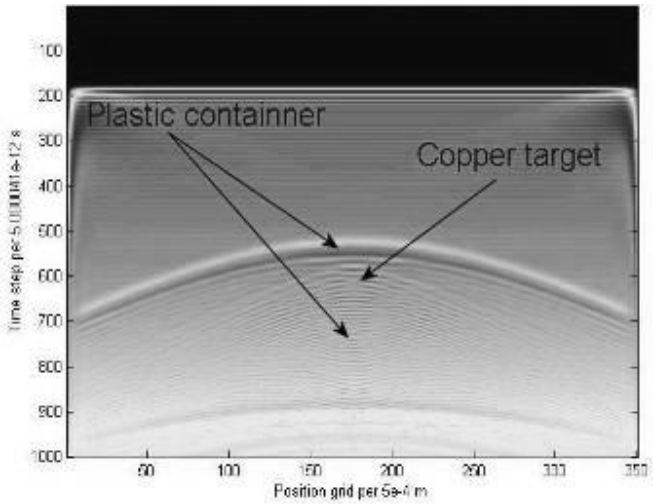

Figure 4. Electric field distribution when backscattered wave reaches the position at which an incident wave was launched.

Figure 4 shows the field distribution at the time the reflected waves reach the signal launch position.

The obtained image shows that the back scattered wave (from the target) is obscured by other waves caused by reflections and scattering in the phantom. Much a clearer picture of the backscattered wave is obtained by subtracting the electric field distribution obtained without the target inside the phantom, as shown in Figure 5.

The remaining results, as presented in Figure 6, concern the second phantom, which assumes more realistic dielectric properties of the breast. The results

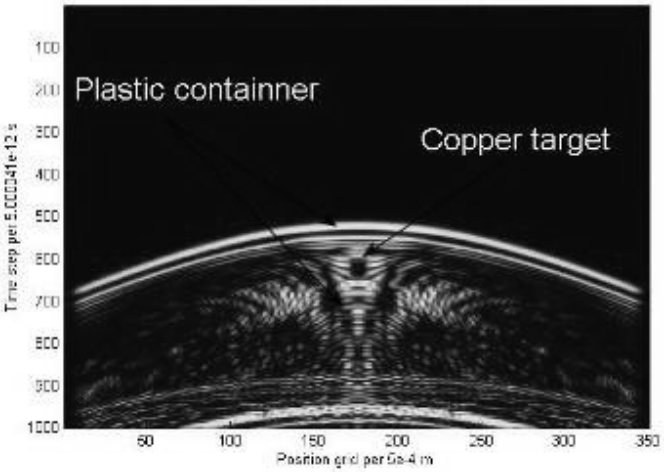

Figure 5. A backscattered signal obtained after by subtracting the electric field distribution for without the target case.

shown in Figure 6 reveal that the reflection from the air-skin interface is dominant.

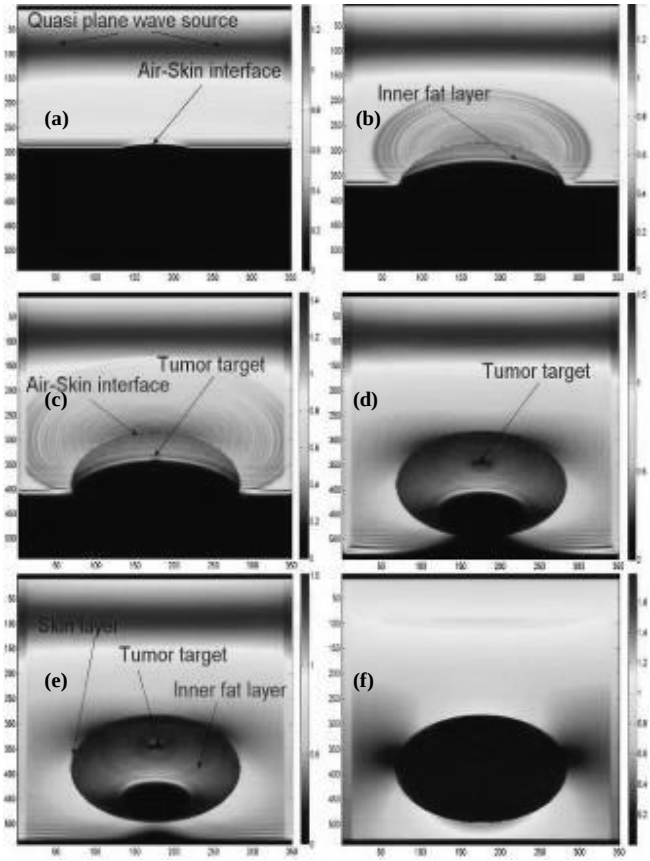

Figure 6. Wave propagation process within the breast phantom.

The wave reflected and scattered from the small tumor tissue is seen inside the phantom region, as shown in

Figure 6(d),(e). However, it is obscured outside the phantom by the wave representing the scattering at the skin interface (Fig. 6(f)).

4. Conclusion

In this paper, two phantoms have been analyzed with the FDTD algorithm to investigate the capability of an ultra-wide band microwave radar system for detection and location of breast tumor. The first phantom is a circular cylindrical plastic container with liquid and a small highly reflecting target. The other one is a three-dimensional numerical breast model obtained from the MR imagery. I order to accelerate computations an FDTD algorithm for use on a cluster of parallel processors has been developed. Numerical calculations have been performed to investigate the phenomenon of wave reflection and scattering in various layers of the two phantoms. In all of the carried out computer simulations, an incident wave in the form of a quasi planar wave has been assumed. Future work will concern other types of waves having capability of focussing on the target to achieve a better quality detection of the malignant tissues.

5. References

[1] K.L Carr, "Microwave radiometry: Its importance to the detection of cancer", *IEEE Trans. Microwave Theory and Tech.*, vol. 37, no. 12, pp. 1862-1869, Dec. 1989.

[2] B. Bocquet et al., "Microwave radiometric imaging at 3GHz for the exploration of breast tumors", *IEEE Trans. Microwave Theory and Tech.*, vol. 38, no. 6, pp. 7910793, June 1990.

[3] L.V. Wang et al.,"Microwave-induced acoustic imaging for biological tissues", Rev. Sci. Instrum., vol. 70, pp. 3744-3748, 1999.

[4] A. E. Bulyshev, S. Y. Semenov, A. E. Souvorov, R. H. Svenson, A. G. Nazarov, Y. E. Sizov, and G. P. Tatsis, "Computational modelling of three-dimensional microwave tomography of breast cancer," *IEEE Trans. Biomed. Eng.*, vol. 48, no. 9, pp. 1053–1056, Sep. 2001.

[5] E. C. Fear, X. Li, S. C. Hagness, and M. A. Stuchly, "Confocal microwave imaging for breast tumor detection: Localization in three dimensions," *IEEE. Trans. Biomed. Eng.*, vol. 49, no. 8, pp. 812–822, Aug. 2002.

[6] E. J. Bond, X. Li, S. C. Hagness, and B. D. Van Veen, "Microwave imaging via space-time beamforming for early detection of breast cancer," *IEEE Trans. Antennas Propag.*, vol. 51, no. 8, pp. 1690–1705, Aug. 2003.

[7] P. Kosmas and C. M. Rappaport, "Time reversal with the FDTD method for microwave breast cancer detection," *IEEE Trans. Microwave Theory and Tech.*, vol. 53, no. 7, pp. 2317–2323, July 2005.

[8] E. C. Fear, P. M. Meaney, and M. A. Stuchly, "Microwaves for breast cancer detection?," *IEEE Potentials*, vol. 22, pp. 12–18, 2003.

[9] M. Converse, E. J. Bond, S. C. Hagness, and B. D. Van Veen, "Ultrawideband microwave space-time beamforming for hyperthermia treatment of breast cancer: A computational feasibility study," *IEEE Trans. Microw. Theory Tech.*, vol. 52, no. 8, pp. 1876–1889, Aug. 2004.

[10] X. Li, S. K. Davis, S. C. Hagness, D. W. van der Weide, and B. D. Van Veen, "Microwave imaging via space–time beamforming: Experimental investigation of tumor detection in multilayer breast phantoms," *IEEE Trans. Microwave Theory Tech.*, vol. 52, pp. 1856–1865, Aug. 2004.

[11] S. Gabriel, R. W. Lau, and C. Gabriel, "The dielectric properties of biological tissues: 11. Measurements on the frequency range 10 Hz to 20 GHz," *Phys. Med. Biol.*, vol. 41, pp. 2251-2269, Nov. 1996.

[12] C. Gabriel, S. Gabriel, and E. Corthout, "The dielectric properties of biological tissues: I. Literature survey," *Phys. Med. Biol.*, vol. 41, pp. 2231-2249, Nov. 1996.

[13] W. T. Joines, Y. 2. Dhenxing, and R. L. Jirtle, "The measured electrical properties of normal and malignant human tissues from 50 to 900 MHz," *Med. Phys.*, vol. 21, pp. 547-550, Apr. 1994.

[14] K. S. Yee, "Numerical solution of initial boundary value problems involving Maxwell's equations in isotropic media," IEEE Trans. Antennas Propagation., Vol. AP-14, pp. 302-307, 1966.

[15] A. C. Cangellaris and D. B. Wright, "Analysis of the numerical error caused by the stair-stepped approximation of a conducting boundary in FDTD simulations of electromagnetic phenomena," IEEE Trans. Antennas Propagation., Vol. 39, pp. 1518-1525, Oct. 1991.

[16] J. P. Berenger, "A Perfectly matched layer for the absorption of electromagnetic waves," Journal of Computational Physics., Vol. 114, pp. 185-200, 1994.

[17] C. Guiffaut and K. Mahdjoubi, "A parallel FDTD algorithm using the MPI library," IEEE Antennas and Propagation Magazine, Vol. 43, No. 2, 2001.

[18] M.E. Bialkowski, W.C. Khor, W.C., and S. Crozier, "A planar microwave imaging system with step-frequency synthesized pulse using different calibration methods", Microwave and Optical Technology Letters, vol. 48, No. 3, pp. 511-516, March 2006.